Fermilab-Pub-12/020-E

arXiv:1201.5172v1 [hep-ex] 25 Jan 2012

Measurement of the top quark mass in $p\bar{p}$ collisions using events with two leptons

V.M. Abazov,[34] B. Abbott,[72] B.S. Acharya,[28] M. Adams,[48] T. Adams,[46] G.D. Alexeev,[34] G. Alkhazov,[38] A. Alton[a],[60] G. Alverson,[59] M. Aoki,[47] A. Askew,[46] B. Åsman,[40] S. Atkins,[57] O. Atramentov,[64] K. Augsten,[9] C. Avila,[7] J. BackusMayes,[79] F. Badaud,[12] L. Bagby,[47] B. Baldin,[47] D.V. Bandurin,[46] S. Banerjee,[28] E. Barberis,[59] P. Baringer,[55] J. Barreto,[3] J.F. Bartlett,[47] U. Bassler,[17] V. Bazterra,[48] A. Bean,[55] M. Begalli,[3] C. Belanger-Champagne,[40] L. Bellantoni,[47] S.B. Beri,[26] G. Bernardi,[16] R. Bernhard,[21] I. Bertram,[41] M. Besançon,[17] R. Beuselinck,[42] V.A. Bezzubov,[37] P.C. Bhat,[47] S. Bhatia,[62] V. Bhatnagar,[26] G. Blazey,[49] S. Blessing,[46] K. Bloom,[63] A. Boehnlein,[47] D. Boline,[69] E.E. Boos,[36] G. Borissov,[41] T. Bose,[58] A. Brandt,[75] O. Brandt,[22] R. Brock,[61] G. Brooijmans,[67] A. Bross,[47] D. Brown,[16] J. Brown,[16] X.B. Bu,[47] M. Buehler,[47] V. Buescher,[23] V. Bunichev,[36] S. Burdin[b],[41] T.H. Burnett,[79] C.P. Buszello,[40] B. Calpas,[14] E. Camacho-Pérez,[31] M.A. Carrasco-Lizarraga,[55] B.C.K. Casey,[47] H. Castilla-Valdez,[31] S. Chakrabarti,[69] D. Chakraborty,[49] K.M. Chan,[53] A. Chandra,[77] E. Chapon,[17] G. Chen,[55] S. Chevalier-Théry,[17] D.K. Cho,[74] S.W. Cho,[30] S. Choi,[30] B. Choudhary,[27] S. Cihangir,[47] D. Claes,[63] J. Clutter,[55] M. Cooke,[47] W.E. Cooper,[47] M. Corcoran,[77] F. Couderc,[17] M.-C. Cousinou,[14] A. Croc,[17] D. Cutts,[74] A. Das,[44] G. Davies,[42] S.J. de Jong,[33] E. De La Cruz-Burelo,[31] F. Déliot,[17] R. Demina,[68] D. Denisov,[47] S.P. Denisov,[37] S. Desai,[47] C. Deterre,[17] K. DeVaughan,[63] H.T. Diehl,[47] M. Diesburg,[47] P.F. Ding,[43] A. Dominguez,[63] T. Dorland,[79] A. Dubey,[27] L.V. Dudko,[36] D. Duggan,[64] A. Duperrin,[14] S. Dutt,[26] A. Dyshkant,[49] M. Eads,[63] D. Edmunds,[61] J. Ellison,[45] V.D. Elvira,[47] Y. Enari,[16] H. Evans,[51] A. Evdokimov,[70] V.N. Evdokimov,[37] G. Facini,[59] T. Ferbel,[68] F. Fiedler,[23] F. Filthaut,[33] W. Fisher,[61] H.E. Fisk,[47] M. Fortner,[49] H. Fox,[41] S. Fuess,[47] A. Garcia-Bellido,[68] G.A. García-Guerra[c],[31] V. Gavrilov,[35] P. Gay,[12] W. Geng,[14,61] D. Gerbaudo,[65] C.E. Gerber,[48] Y. Gershtein,[64] G. Ginther,[47,68] G. Golovanov,[34] A. Goussiou,[79] P.D. Grannis,[69] S. Greder,[18] H. Greenlee,[47] Z.D. Greenwood,[57] E.M. Gregores,[4] G. Grenier,[19] Ph. Gris,[12] J.-F. Grivaz,[15] A. Grohsjean[d],[17] S. Grünendahl,[47] M.W. Grünewald,[29] T. Guillemin,[15] G. Gutierrez,[47] P. Gutierrez,[72] A. Haas[e],[67] S. Hagopian,[46] J. Haley,[59] L. Han,[6] K. Harder,[43] A. Harel,[68] J.M. Hauptman,[54] J. Hays,[42] T. Head,[43] T. Hebbeker,[20] D. Hedin,[49] H. Hegab,[73] A.P. Heinson,[45] U. Heintz,[74] C. Hensel,[22] I. Heredia-De La Cruz,[31] K. Herner,[60] G. Hesketh[f],[43] M.D. Hildreth,[53] R. Hirosky,[78] T. Hoang,[46] J.D. Hobbs,[69] B. Hoeneisen,[11] M. Hohlfeld,[23] Z. Hubacek,[9,17] V. Hynek,[9] I. Iashvili,[66] Y. Ilchenko,[76] R. Illingworth,[47] A.S. Ito,[47] S. Jabeen,[74] M. Jaffré,[15] D. Jamin,[14] A. Jayasinghe,[72] R. Jesik,[42] K. Johns,[44] M. Johnson,[47] A. Jonckheere,[47] P. Jonsson,[42] J. Joshi,[26] A.W. Jung,[47] A. Juste,[39] K. Kaadze,[56] E. Kajfasz,[14] D. Karmanov,[36] P.A. Kasper,[47] I. Katsanos,[63] R. Kehoe,[76] S. Kermiche,[14] N. Khalatyan,[47] A. Khanov,[73] A. Kharchilava,[66] Y.N. Kharzheev,[34] J.M. Kohli,[26] A.V. Kozelov,[37] J. Kraus,[61] S. Kulikov,[37] A. Kumar,[66] A. Kupco,[10] T. Kurča,[19] V.A. Kuzmin,[36] S. Lammers,[51] G. Landsberg,[74] P. Lebrun,[19] H.S. Lee,[30] S.W. Lee,[54] W.M. Lee,[47] J. Lellouch,[16] H. Li,[13] L. Li,[45] Q.Z. Li,[47] S.M. Lietti,[5] J.K. Lim,[30] D. Lincoln,[47] J. Linnemann,[61] V.V. Lipaev,[37] R. Lipton,[47] Y. Liu,[6] A. Lobodenko,[38] M. Lokajicek,[10] R. Lopes de Sa,[69] H.J. Lubatti,[79] R. Luna-Garcia[g],[31] A.L. Lyon,[47] A.K.A. Maciel,[2] D. Mackin,[77] R. Madar,[17] R. Magaña-Villalba,[31] S. Malik,[63] V.L. Malyshev,[34] Y. Maravin,[56] J. Martínez-Ortega,[31] R. McCarthy,[69] C.L. McGivern,[55] M.M. Meijer,[33] A. Melnitchouk,[62] D. Menezes,[49] P.G. Mercadante,[4] M. Merkin,[36] A. Meyer,[20] J. Meyer,[22] F. Miconi,[18] N.K. Mondal,[28] G.S. Muanza,[14] M. Mulhearn,[78] E. Nagy,[14] M. Naimuddin,[27] M. Narain,[74] R. Nayyar,[27] H.A. Neal,[60] J.P. Negret,[7] P. Neustroev,[38] S.F. Novaes,[5] T. Nunnemann,[24] G. Obrant[‡],[38] J. Orduna,[77] N. Osman,[14] J. Osta,[53] G.J. Otero y Garzón,[1] M. Padilla,[45] A. Pal,[75] N. Parashar,[52] V. Parihar,[74] S.K. Park,[30] R. Partridge[e],[74] N. Parua,[51] A. Patwa,[70] B. Penning,[47] M. Perfilov,[36] Y. Peters,[43] K. Petridis,[43] G. Petrillo,[68] P. Pétroff,[15] R. Piegaia,[1] M.-A. Pleier,[70] P.L.M. Podesta-Lerma[h],[31] V.M. Podstavkov,[47] P. Polozov,[35] A.V. Popov,[37] M. Prewitt,[77] D. Price,[51] N. Prokopenko,[37] J. Qian,[60] A. Quadt,[22] B. Quinn,[62] M.S. Rangel,[2] K. Ranjan,[27] P.N. Ratoff,[41] I. Razumov,[37] P. Renkel,[76] M. Rijssenbeek,[69] I. Ripp-Baudot,[18] F. Rizatdinova,[73] M. Rominsky,[47] A. Ross,[41] C. Royon,[17] P. Rubinov,[47] R. Ruchti,[53] G. Safronov,[35] G. Sajot,[13] P. Salcido,[49] A. Sánchez-Hernández,[31] M.P. Sanders,[24] B. Sanghi,[47] A.S. Santos,[5] G. Savage,[47] L. Sawyer,[57] T. Scanlon,[42] R.D. Schamberger,[69] Y. Scheglov,[38] H. Schellman,[50] T. Schliephake,[25] S. Schlobohm,[79] C. Schwanenberger,[43] R. Schwienhorst,[61] J. Sekaric,[55] H. Severini,[72] E. Shabalina,[22] V. Shary,[17] A.A. Shchukin,[37] R.K. Shivpuri,[27] V. Simak,[9] V. Sirotenko,[47] P. Skubic,[72] P. Slattery,[68] D. Smirnov,[53] K.J. Smith,[66] G.R. Snow,[63] J. Snow,[71] S. Snyder,[70] S. Söldner-Rembold,[43] L. Sonnenschein,[20] K. Soustruznik,[8] J. Stark,[13] V. Stolin,[35] D.A. Stoyanova,[37] M. Strauss,[72] D. Strom,[48] L. Stutte,[47] L. Suter,[43] P. Svoisky,[72] M. Takahashi,[43] A. Tanasijczuk,[1] M. Titov,[17] V.V. Tokmenin,[34] Y.-T. Tsai,[68] K. Tschann-Grimm,[69] D. Tsybychev,[69] B. Tuchming,[17] C. Tully,[65] L. Uvarov,[38]

S. Uvarov,[38] S. Uzunyan,[49] R. Van Kooten,[51] W.M. van Leeuwen,[32] N. Varelas,[48] E.W. Varnes,[44] I.A. Vasilyev,[37] P. Verdier,[19] L.S. Vertogradov,[34] M. Verzocchi,[47] M. Vesterinen,[43] D. Vilanova,[17] P. Vokac,[9] H.D. Wahl,[46] M.H.L.S. Wang,[47] J. Warchol,[53] G. Watts,[79] M. Wayne,[53] M. Weber[i],[47] J. Weichert,[23] L. Welty-Rieger,[50] A. White,[75] D. Wicke,[25] M.R.J. Williams,[41] G.W. Wilson,[55] M. Wobisch,[57] D.R. Wood,[59] T.R. Wyatt,[43] Y. Xie,[47] R. Yamada,[47] W.-C. Yang,[43] T. Yasuda,[47] Y.A. Yatsunenko,[34] W. Ye,[69] Z. Ye,[47] H. Yin,[47] K. Yip,[70] S.W. Youn,[47] T. Zhao,[79] B. Zhou,[60] J. Zhu,[60] M. Zielinski,[68] D. Zieminska,[51] and L. Zivkovic[74]

(The D0 Collaboration)*

[1] *Universidad de Buenos Aires, Buenos Aires, Argentina*
[2] *LAFEX, Centro Brasileiro de Pesquisas Físicas, Rio de Janeiro, Brazil*
[3] *Universidade do Estado do Rio de Janeiro, Rio de Janeiro, Brazil*
[4] *Universidade Federal do ABC, Santo André, Brazil*
[5] *Instituto de Física Teórica, Universidade Estadual Paulista, São Paulo, Brazil*
[6] *University of Science and Technology of China, Hefei, People's Republic of China*
[7] *Universidad de los Andes, Bogotá, Colombia*
[8] *Charles University, Faculty of Mathematics and Physics, Center for Particle Physics, Prague, Czech Republic*
[9] *Czech Technical University in Prague, Prague, Czech Republic*
[10] *Center for Particle Physics, Institute of Physics, Academy of Sciences of the Czech Republic, Prague, Czech Republic*
[11] *Universidad San Francisco de Quito, Quito, Ecuador*
[12] *LPC, Université Blaise Pascal, CNRS/IN2P3, Clermont, France*
[13] *LPSC, Université Joseph Fourier Grenoble 1, CNRS/IN2P3, Institut National Polytechnique de Grenoble, Grenoble, France*
[14] *CPPM, Aix-Marseille Université, CNRS/IN2P3, Marseille, France*
[15] *LAL, Université Paris-Sud, CNRS/IN2P3, Orsay, France*
[16] *LPNHE, Universités Paris VI and VII, CNRS/IN2P3, Paris, France*
[17] *CEA, Irfu, SPP, Saclay, France*
[18] *IPHC, Université de Strasbourg, CNRS/IN2P3, Strasbourg, France*
[19] *IPNL, Université Lyon 1, CNRS/IN2P3, Villeurbanne, France and Université de Lyon, Lyon, France*
[20] *III. Physikalisches Institut A, RWTH Aachen University, Aachen, Germany*
[21] *Physikalisches Institut, Universität Freiburg, Freiburg, Germany*
[22] *II. Physikalisches Institut, Georg-August-Universität Göttingen, Göttingen, Germany*
[23] *Institut für Physik, Universität Mainz, Mainz, Germany*
[24] *Ludwig-Maximilians-Universität München, München, Germany*
[25] *Fachbereich Physik, Bergische Universität Wuppertal, Wuppertal, Germany*
[26] *Panjab University, Chandigarh, India*
[27] *Delhi University, Delhi, India*
[28] *Tata Institute of Fundamental Research, Mumbai, India*
[29] *University College Dublin, Dublin, Ireland*
[30] *Korea Detector Laboratory, Korea University, Seoul, Korea*
[31] *CINVESTAV, Mexico City, Mexico*
[32] *Nikhef, Science Park, Amsterdam, the Netherlands*
[33] *Radboud University Nijmegen, Nijmegen, the Netherlands and Nikhef, Science Park, Amsterdam, the Netherlands*
[34] *Joint Institute for Nuclear Research, Dubna, Russia*
[35] *Institute for Theoretical and Experimental Physics, Moscow, Russia*
[36] *Moscow State University, Moscow, Russia*
[37] *Institute for High Energy Physics, Protvino, Russia*
[38] *Petersburg Nuclear Physics Institute, St. Petersburg, Russia*
[39] *Institució Catalana de Recerca i Estudis Avançats (ICREA) and Institut de Física d'Altes Energies (IFAE), Barcelona, Spain*
[40] *Stockholm University, Stockholm and Uppsala University, Uppsala, Sweden*
[41] *Lancaster University, Lancaster LA1 4YB, United Kingdom*
[42] *Imperial College London, London SW7 2AZ, United Kingdom*
[43] *The University of Manchester, Manchester M13 9PL, United Kingdom*
[44] *University of Arizona, Tucson, Arizona 85721, USA*
[45] *University of California Riverside, Riverside, California 92521, USA*
[46] *Florida State University, Tallahassee, Florida 32306, USA*
[47] *Fermi National Accelerator Laboratory, Batavia, Illinois 60510, USA*
[48] *University of Illinois at Chicago, Chicago, Illinois 60607, USA*
[49] *Northern Illinois University, DeKalb, Illinois 60115, USA*
[50] *Northwestern University, Evanston, Illinois 60208, USA*
[51] *Indiana University, Bloomington, Indiana 47405, USA*
[52] *Purdue University Calumet, Hammond, Indiana 46323, USA*

[53] *University of Notre Dame, Notre Dame, Indiana 46556, USA*
[54] *Iowa State University, Ames, Iowa 50011, USA*
[55] *University of Kansas, Lawrence, Kansas 66045, USA*
[56] *Kansas State University, Manhattan, Kansas 66506, USA*
[57] *Louisiana Tech University, Ruston, Louisiana 71272, USA*
[58] *Boston University, Boston, Massachusetts 02215, USA*
[59] *Northeastern University, Boston, Massachusetts 02115, USA*
[60] *University of Michigan, Ann Arbor, Michigan 48109, USA*
[61] *Michigan State University, East Lansing, Michigan 48824, USA*
[62] *University of Mississippi, University, Mississippi 38677, USA*
[63] *University of Nebraska, Lincoln, Nebraska 68588, USA*
[64] *Rutgers University, Piscataway, New Jersey 08855, USA*
[65] *Princeton University, Princeton, New Jersey 08544, USA*
[66] *State University of New York, Buffalo, New York 14260, USA*
[67] *Columbia University, New York, New York 10027, USA*
[68] *University of Rochester, Rochester, New York 14627, USA*
[69] *State University of New York, Stony Brook, New York 11794, USA*
[70] *Brookhaven National Laboratory, Upton, New York 11973, USA*
[71] *Langston University, Langston, Oklahoma 73050, USA*
[72] *University of Oklahoma, Norman, Oklahoma 73019, USA*
[73] *Oklahoma State University, Stillwater, Oklahoma 74078, USA*
[74] *Brown University, Providence, Rhode Island 02912, USA*
[75] *University of Texas, Arlington, Texas 76019, USA*
[76] *Southern Methodist University, Dallas, Texas 75275, USA*
[77] *Rice University, Houston, Texas 77005, USA*
[78] *University of Virginia, Charlottesville, Virginia 22901, USA*
[79] *University of Washington, Seattle, Washington 98195, USA*

(Dated: January 24, 2012)

We present a measurement of the top quark mass (m_t) in $p\bar{p}$ collisions at $\sqrt{s} = 1.96$ TeV using $t\bar{t}$ events with two leptons (ee, $e\mu$ or $\mu\mu$) in the final state in 4.3 fb^{-1} of data collected with the D0 detector at the Fermilab Tevatron collider. We analyze the kinematically underconstrained dilepton events by integrating over the neutrino rapidity distributions. We reduce the dominant systematic uncertainties from jet energy calibration using a correction obtained from $t\bar{t}\to\ell$+jets events. We also correct jets in simulated events to replicate the quark flavor dependence of the jet response in data. In combination with our previous analysis [1], we measure $m_t = 174.0 \pm 2.4(\text{stat}) \pm 1.4(\text{syst})$ GeV.

PACS numbers: 12.15.Ff, 14.65.Ha

The masses of fundamental fermions in the standard model (SM) are generated through their interaction with a hypothesized scalar Higgs field with a strength given by a Yukawa coupling specific to each fermion species. The Yukawa coupling of the top quark is 1 within uncertainties, and this value is directly constrained by a measurement of the top quark mass. Recent direct searches for the SM Higgs boson have excluded a substantial part of the allowed mass range [2–4] without yielding a discovery. It is important to sharpen the prediction for the Higgs boson mass. This requires precise measurements of the W boson mass, M_W, and the top quark mass, m_t, since the masses of these three particles are connected in the SM through radiative corrections.

In $p\bar{p}$ collisions, top quarks t are primarily produced in $t\bar{t}$ pairs, with each t quark decaying predominantly to b quarks with $BR(t \to Wb) \sim 100\%$. These events yield final states with either 0, 1, or 2 leptons from the decays of the two W bosons coming from $t\bar{t}$ decay. We consider here the dilepton channel where the two leptons are electrons or muons of large transverse momentum, p_T. We analyzed such dilepton events using previously collected data [1, 5] with the neutrino weighting (νWT) approach [6]. While the dilepton channel has low backgrounds, the small branching ratio into leptons means that m_t measurements from these events were statistically limited until recently [7]. In addition, dominant systematic uncertainties from jet energy calibration have been large [1] in this channel compared to the channel with one lepton and four or more jets (ℓ+jets). In ℓ+jets events, two quarks originating from W boson decay yield a dijet mass signature that permits a precise calibration of jet energies for the mass measurement in $t\bar{t}$ events [8]. In this Letter, we present a new measurement of m_t using the D0 detector with 4.3 fb^{-1} of $p\bar{p}$ collider data in the ee,

* with visitors from [a]Augustana College, Sioux Falls, SD, USA, [b]The University of Liverpool, Liverpool, UK, [c]UPIITA-IPN, Mexico City, Mexico, [d]DESY, Hamburg, Germany, [e]SLAC, Menlo Park, CA, USA, [f]University College London, London, UK, [g]Centro de Investigacion en Computacion - IPN, Mexico City, Mexico, [h]ECFM, Universidad Autonoma de Sinaloa, Culiacán, Mexico, and [i]Universität Bern, Bern, Switzerland. [‡]Deceased.

$e\mu$, and $\mu\mu$ final states. We improve the jet calibration by using the energy scale derived in ℓ+jets events [9]. Our approach differs from [10] in that we do not use the ℓ+jets scale constraint through a combined fit of the ℓ+jets and dilepton events. Instead we use the calibration obtained from the ℓ+jets events and carefully estimate the uncertainties originating from the use of that calibration in a different environment. This demonstrates how the calibration obtained using the dijet constraint from M_W can be applied to different final states.

The D0 detector [11] is a multipurpose detector operated at the Fermilab Tevatron $p\bar{p}$ collider. The inner detector consists of coaxial cylinders and disks of silicon microstrips for track and vertex reconstruction. Eight layers of scintillating fibers arranged in doublets surround the silicon microstrip tracker to provide further tracking measurements out to forward pseudorapidities, η [12]. A 1.9 T solenoid produces a magnetic field for the tracking detectors. Uranium-liquid argon calorimeters surround the tracking volume and perform both electromagnetic and hadronic shower energy measurements. Thin scintillation inter-cryostat detectors provide shower sampling in the region between the central and endcap calorimeters. Three layers of proportional drift tubes and scintillation counters reside outside the calorimetry, with 1.8 T toroids that provide muon identification and independent measurement of muon momenta.

We simulate $t\bar{t}$ events using Monte Carlo (MC) samples for 140 GeV $< m_t <$ 200 GeV using the ALPGEN generator [13] and PYTHIA [14] for parton fragmentation. Backgrounds originate from $Z/\gamma^* \to 2\ell$+jets and $WW/WZ/ZZ \to 2\ell$+jets production. For the former we use ALPGEN plus PYTHIA, while diboson backgrounds are simulated with PYTHIA. We pass all MC events through a full detector simulation based on GEANT [15]. Backgrounds from instrumental effects that result in misidentified leptons are modeled using data.

We use single and two lepton triggers to select events used in this analysis. Data and simulated events are reconstructed to provide the momenta of tracks, jets, and lepton candidates. Charged leptons are required to be isolated from other calorimeter energy deposits, and to have an associated track in the inner detector. Calorimeter shower and tracking information are used to identify electrons. Track parameters in the muon and inner detector system are used to identify muons. We reconstruct jets with an iterative, midpoint cone algorithm with radius $\mathcal{R}_{\rm cone} = 0.5$ [16]. Jets are calibrated with the standard D0 jet energy scale method [17], which corrects to the jet energy measured with the same cone algorithm applied to particles from jet fragmentation before they interact with the detector. The jets in data and MC are calibrated independently so that their relative response is close to 1. This corrects for detector response, energy deposited outside of the jet cone, electronics noise, and pileup. The largest correction compensates for the detector response, and is extracted using γ+jet events in data and MC. We also correct jets for the p_T of any embedded muon plus that of the associated neutrino. We initially apply the standard calibration because it provides detailed p_T and η dependent corrections. It also provides distinct corrections to jets and the imbalance in event missing transverse energy, $\not\!\!E_T$, because several components (e.g. noise and out-of-cone effects) result from the jet reconstruction algorithm rather than any undetected energy. In the p_T range of jets found in $t\bar{t}$ events, the uncertainty of the standard D0 jet energy calibration averages 2% and is dominated by systematic effects. We use responses of single particles from data and MC to determine the energy scale for different jet flavors. We correct MC jets by the ratio of data response to MC response according to their flavor to ensure that the MC reflects the flavor dependence in data, as in [9]. We calculate $\not\!\!E_T$ as the negative of the vector sum of all transverse components of calorimeter cell energies and muon track momenta, corrected for the response to electrons and jets.

Events are selected to have two leptons (ee, $e\mu$, $\mu\mu$) and two or more jets. The leptons must have $p_T >$ 15 GeV and the jets must have $p_T > 20$ GeV. Electrons and jets are required to satisfy $|\eta| < 2.5$, while muons must have $|\eta| < 2$. We further require $\not\!\!E_T >$ 40 GeV in the $\mu\mu$ channel. The $e\mu$ events must satisfy $H_T > 120$ GeV, where H_T is defined to be the sum of the p_Ts of jets and the leading lepton. In $\mu\mu$ and ee events, we further require $\not\!\!E_T$ to be significantly different than typical values found in the distribution from Z boson events. These and all other selections are detailed in [18]. We observe 50, 198, and 84 events with expected background yields of 10.4, 28.1, and 31.0 events in the ee, $e\mu$, and $\mu\mu$ channels, respectively.

In ℓ+jets events, one W boson decays to two quarks which fragment to jets. The invariant mass of this jet pair can be used to improve the calibration for all jets in these events. Complications arise because the four jets in the ℓ+jets events can be incorrectly assigned to the initial four quarks. Energy from different partons is also mixed in the same jet due to a high jet multiplicity. Observed jet energies are also affected by color flow effects, which are different for the b-quark jets and for jets from the decay of color singlet W bosons. These attributes are specific to a particular event topology such as ℓ+jets. Nevertheless, a scale factor based on the dijet invariant mass that is correlated with M_W can be extracted. The most recent analysis of this kind by D0 used 2.6 fb^{-1} of data and obtained a calibration factor of 1.013 ± 0.008(stat) [9]. The uncertainty of 0.8% is substantially smaller than that of the standard jet energy correction and will decrease with additional data.

The jet multiplicity is different in dilepton (2ℓ) and ℓ+jets events. In order to carry over the ℓ+jets calibration, we must consider the possibility that the energy scale of the b-quark jets in the two channels can differ. We calculate the energy scale, $R^{2\ell}$, for MC b-quark jets in the dilepton sample using known responses for single particles that fall within the reconstructed jet

cone. We calculate this response using single particle responses from data, giving $R^{2\ell}_{\rm data}$, and using particle responses from MC, giving $R^{2\ell}_{\rm MC}$. We calculate the ratio of these two responses, and the analogous ratio for MC b-quark jets in the ℓ+jets sample. The ratio of these two ratios

$$\mathcal{R}^b_{2\ell}(p^b_T) = \frac{R^{2\ell}_{\rm data}(p^b_T)/R^{2\ell}_{\rm MC}(p^b_T)}{R^{\ell+\rm jets}_{\rm data}(p^b_T)/R^{\ell+\rm jets}_{\rm MC}(p^b_T)}, \qquad (1)$$

varies between 1.001 and 1.003 depending on b-quark jet p_T, p^b_T. The particle multiplicity of b-quark jets in ℓ+jets events is a few percent higher than in the dilepton sample, which is a sufficiently large difference to account for the observed value of $\mathcal{R}^b_{2\ell}$. Therefore, we take 0.3% from the maximum excursion of $\mathcal{R}^b_{2\ell}$ from unity as a systematic uncertainty on carrying over the ℓ+jets scale to the jets in our dilepton sample, which we apply as a direct correction in addition to the standard calibration.

The jet energy scale calibration obtained in [9] is based on a subset of the data used for this analysis and therefore we have to estimate the effect of using the calibration on a larger data set. The instantaneous luminosity of the dilepton sample is higher on average. We reweight the distribution of the number of primary vertices in the ℓ+jets sample to match the distribution in the 4.3 fb^{-1} ℓ+jets data and recalculate the ℓ+jets energy scale. This produces a negligible effect. To account for a possible shift in the energy scale of the liquid argon calorimeter, we apply a correction derived from 4.3 fb^{-1} rather than 2.6 fb^{-1}, and this yields a 0.7% shift in jet energy scale. From these studies, we obtain a total uncertainty on the ℓ+jets energy scale as applied to our analysis as the sum in quadrature of the statistical uncertainty (0.8%), $\mathcal{R}^b_{2\ell}$ (0.3%), and the calorimeter calibration (0.7%). This yields a 1.1% uncertainty when applying the ℓ+jets energy scale.

The consequence of two neutrinos in dilepton events is an underconstrained kinematics. We employ the νWT technique to extract m_t [6] due to its weak dependence on the modeling details of $t\bar{t}$ events. We integrate over the η distributions of both neutrinos and solve the event kinematics to allow a calculation of $\not\!\!E_T$ from the neutrino momentum solutions. We have increased the sampling for this integration by an order of magnitude relative to our previous analysis [1], which improves the expected statistical uncertainty on m_t by 4%. By comparing the calculated $\not\!\!E_T$ to the measured $\not\!\!E_T$ for each event, we calculate a weight for a given m_t. For each neutrino rapidity sampling, we sum the weight values calculated from all combinations of neutrino momentum solutions and jet assignments. We therefore arrive at a distribution of relative weight for a range of m_t for each event. Requiring the integral of this distribution to be nonzero excludes events with a measured $\not\!\!E_T$ that is incompatible with coming from neutrinos from top quark decay. This introduces a small inefficiency for the $t\bar{t}$ signal and reduces the background contamination in the final sample. Our final kinematically reconstructed data sample consists of 49, 190, and 80 events in the ee, $e\mu$, and $\mu\mu$ channels, respectively.

TABLE I. Calibration parameters for the analysis of ee, $e\mu$, and $\mu\mu$ channels and the combination of these channels.

Channel	Slope	Offset [GeV]	Pull width
ee	0.976 ± 0.014	0.03 ± 0.16	1.01 ± 0.01
$e\mu$	0.973 ± 0.012	0.43 ± 0.14	1.03 ± 0.01
$\mu\mu$	1.038 ± 0.022	0.49 ± 0.23	1.06 ± 0.03

Probability distributions of the mean and RMS values (μ_w and σ_w, respectively) of the event weight distributions are constructed for background in each channel. Each background component is normalized to its expected event yield. We generate distributions of $t\bar{t}$ signal probability as a function of μ_w, σ_w, and m_t. We perform a binned maximum likelihood fit of an analyzed event sample to these probability distributions according to the total signal and background yields expected in our data. The signal yield is normalized to the calculated cross section for $t\bar{t}$ production [19] evaluated at $m_t = 172.5$ GeV. For all measurements, we obtain a likelihood ($\mathcal{L}$) vs. m_t. We fit a parabola to the $-\ln\mathcal{L}$ vs. m_t, and the fitted mass, $m_t^{\rm fit}$, is defined as the lowest point of the parabola. The $-\ln\mathcal{L}$ vs. m_t for data is shown in Fig. 1. The statistical uncertainty for each measurement is taken as the half-width of the parabola at 0.5 units in $-\ln\mathcal{L}$ above the minimum at $m_t^{\rm fit}$.

The above procedure is followed for the extraction of m_t from data and is used to calibrate the result as follows. We construct pseudoexperiments from signal and background MC samples according to their expected yields and allow fluctuations in each such that the total equals the number of observed events. We perform 1000 pseudoexperiments for each channel and measure $m_t^{\rm fit}$ in each. A linear fit of $m_t^{\rm fit}$ vs. the input m_t provides a calibration for our method. We also calculate the pull width of the average estimated statistical uncertainty vs the RMS of $m_t^{\rm fit}$ values. The resulting slopes, offsets, and pull widths are given in Table I. The $m_t^{\rm fit}$ and estimated statistical uncertainty on the data are corrected with these parameters. We obtain a calibrated mass measurement for the 4.3 fb^{-1} sample in the ee, $e\mu$, and $\mu\mu$ channels.

The largest systematic uncertainties are associated with the jet calibration. We change the ℓ+jets energy scale factor by $\pm$1.1% and perform our analysis to obtain a systematic uncertainty on m_t. This yields an uncertainty of 0.9 GeV. The result of the ℓ+jets analysis is a single scale factor averaged over all jet p_Ts that are utilized in the dijet mass, i.e. dominated by light quark jets from W boson decay. As in [9], we determine an additional uncertainty to account for the difference in p_T distribution for the b-quark jets in dilepton events as compared to jets from the $W \to jj$ sample. To estimate an uncertainty from this difference, we treat the p_T and η dependence of the uncertainty in the standard

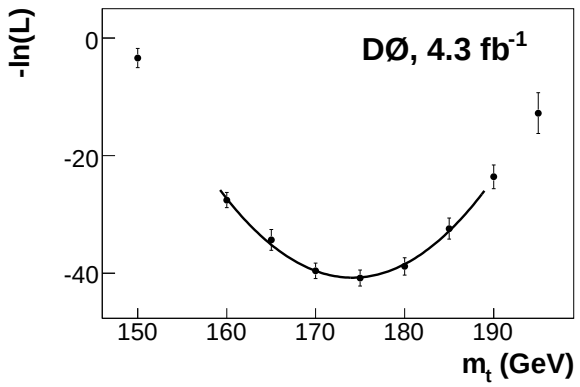

FIG. 1. The $-\ln\mathcal{L}$ vs. m_t for the combination of ee, $e\mu$, and $\mu\mu$ channels. A parabolic fit near the minimum is shown.

jet energy scale as a possible dependence of the residual energy scale following the calibration to ℓ+jets. We calculate the average of the energy scale uncertainty for jets in dilepton events as follows. For each jet, we apply a shift equal to the difference between its uncertainty in energy scale, normalized to its energy scale, and the sample's average uncertainty in energy scale normalized to that energy scale. Propagating this difference through the mass analysis yields a 0.3 GeV uncertainty on m_t.

The flavor-dependent jet energy corrections described earlier allow our mass templates, which are determined largely from MC samples, to accurately reflect the data. As in [9], we propagate the uncertainty in these corrections and obtain a systematic uncertainty on the top quark mass of 0.5 GeV.

We evaluate the effect of our uncertainty in modeling initial state radiation (ISR) and final state radiation (FSR) by comparing PYTHIA with different ISR and FSR parameters. Color reconnection uncertainties are estimated by comparing the analysis with PYTHIA using two different tunes [20]. Higher order QCD evolution is estimated by comparing the nominal ALPGEN plus PYTHIA configuration with MC@NLO plus HERWIG [21]. To estimate our sensitivity to uncertainties in the parton distribution functions, PDFs, we use the CTEQ6M PDF set to employ the method described in [22].

We modify the jet energy resolution in MC events to reflect the resolution in data. We evaluate the effect of an uncertainty in this oversmearing on the mass measurement by shifting the jet resolution by one standard deviation. We treat the electron and muon energy and momentum scales similarly by shifting their calibrations within uncertainties.

We account for the uncertainty in the method arising from the uncertainties on the offset and slope of the calibration from pseudoexperiments. We also estimate the uncertainty due to the statistics employed in our templates of the probability distribution. We construct 1000 new templates, for both signal and background, and vary their bin contents within their Gaussian uncertainties. With these templates, we obtain 1000 new measurements from data and quote the RMS of these values as a systematic uncertainty. We assign a systematic uncertainty on the signal fraction by shifting the background contributions in pseudoexperiments within their total uncertainty.

TABLE II. Estimated systematic uncertainties on m_t for the combined dilepton measurement.

Source	Uncertainty (GeV)
Jet energy calibration	
Overall scale	0.9
Flavor dependence	0.5
Residual scale	0.3
Signal modeling	
ISR/FSR	0.4
Color reconnection	0.5
Higher order effects	0.6
b quark fragmentation	0.1
PDF uncertainty	0.5
Object reconstruction	
Muon p_T resolution	0.2
Electron energy scale	0.2
Muon p_T scale	0.2
Jet resolution	0.3
Jet identification	0.3
Method	
Calibration	0.1
Template statistics	0.5
Signal fraction	0.2
Total systematic uncertainty	1.5

We combine measurements in the three dilepton channels using the method of best linear unbiased estimator [23]. We calculate each systematic uncertainty for the combined result, as given in Table II, according to its correlation among channels. The resulting measurement gives $m_t = 173.7 \pm 2.8(\text{stat}) \pm 1.5(\text{syst})$ GeV.

We combine this measurement with D0's measurement in the preceding 1 fb^{-1} of data using the νWT and matrix weighting methods [1]. Some uncertainties evaluated in the 4.3 fb^{-1} sample are not available for the 1.0 fb^{-1} sample. In these cases, we add the new uncertainties to the result from the previous analysis. We consider the statistical uncertainties uncorrelated, as well as several systematic uncertainties: calibration of method, template statistics, overall jet energy scale, and flavor dependence ("b-quark/light quark" in the previous analysis). We consider all other uncertainties to be fully correlated. The combined measurement yields $m_t = 174.0 \pm 2.4(\text{stat}) \pm 1.4(\text{syst})$ GeV. This is consistent with measurements in other channels and is the most precise m_t measurement in the dilepton channel to date.

We thank the staffs at Fermilab and collaborating institutions, and acknowledge support from the DOE and NSF (USA); CEA and CNRS/IN2P3 (France);

FASI, Rosatom and RFBR (Russia); CNPq, FAPERJ, FAPESP and FUNDUNESP (Brazil); DAE and DST (India); Colciencias (Colombia); CONACyT (Mexico); NRF (Korea); CONICET and UBACyT (Argentina); FOM (The Netherlands); STFC and the Royal Society (United Kingdom); MSMT and GACR (Czech Republic); BMBF and DFG (Germany); SFI (Ireland); The Swedish Research Council (Sweden); and CAS and CNSF (China).

[1] V. M. Abazov *et al.* (D0 Collaboration), Phys. Rev. D **80**, 092006 (2009).
[2] ALEPH Collaboration, DELPHI Collaboration, L3 Collaboration, OPAL Collaboration, The LEP Working Group for Higgs Boson Sear ches, Phys. Lett. B **565**, 61 (2003).
[3] T. Aaltonen *et al.* (CDF and D0 Collaborations), Phys. Rev. Lett. **104**, 061802 (2010); T. Aaltonen *et al.* (CDF Collaboration), Phys. Rev. Lett. **104**, 061803 (2010); V. M. Abazov *et al.* (D0 Collaboration), Phys. Rev. Lett. **104**, 061804 (2010).
[4] G. Aad *et al.* (ATLAS Collaboration), arXiv:1112.2577 [hep-ex], submitted to Phys. Rev. Lett.; S. Chatrchyan *et al.* (CMS Collaboration), Phys. Lett. B **699**, 25 (2011).
[5] V. M. Abazov *et al.* (D0 Collaboration), Phys. Lett. B **655**, 7 (2007).
[6] S. Abachi *et al.* (D0 Collaboration), Phys. Rev. Lett. **80**, 2063 (1998).
[7] V. M. Abazov *et al.* (D0 Collaboration), Phys. Rev. Lett. **107**, 082004 (2011).
[8] V. M. Abazov *et al.* (D0 Collaboration), Nature **429**, 638 (2004).
[9] V. M. Abazov *et al.* (D0 Collaboration), Phys. Rev. D **84**, 032004 (2011).
[10] T. Aaltonen *et al.* (CDF Collaboration), Phys. Rev. D **83**, 111101 (2011).
[11] V. M. Abazov *et al.* (D0 Collaboration), Nucl. Instrum. Methods in Phys. Res. Sect. A **565**, 463 (2006); S. N. Ahmed *et al.*, Nucl. Instrum. Methods in Phys. Res. Sect. A **634**, 8 (2011); R. Angstadt *et al.*, Nucl. Instrum. Methods in Phys. Res. Sect. A **622**, 298 (2010); M. Abolins *et al.*, Nucl. Instrum. Methods in Phys. Res. Sect. A **584**, 75 (2008).
[12] The pseudorapidity is defined as $\eta = -\ln[\tan(\theta/2)]$ where θ is the polar angle relative to the beam axis, defined relative to the center of the detector.
[13] M. Mangano *et al.*, J. High Energy Phys. **07**, 001 (2003); M. Mangano, M. Moretti and R. Pittau, Nucl. Phys. B **632**, 343 (2002); F. Caravaglios *et al.*, Nucl. Phys. B **539**, 215 (1999).
[14] T. Sjöstrand *et al.*, Comput. Phys. Commun. **135**, 238 (2001).
[15] R. Brun and F. Carminati, CERN Program Library Long Writeup W5013, 1993 (unpublished).
[16] G. Blazey *et al.*, arXiv:hep-ex/0005012 (2000).
[17] V. M. Abazov *et al.* (D0 Collaboration), arXiv:1110.3771v1 [hep-ex] (2011), submitted to Phys. Rev. D; S. Abachi *et al.* (D0 Collaboration), Nucl. Instrum. Methods in Phys. Res. A **424**, 352 (1999).
[18] V. M. Abazov *et al.* (D0 Collaboration), Phys. Lett. B **704**, 403 (2011).
[19] S. Moch and P. Uwer, Phys. Rev. D **78**, 034003 (2008).
[20] A. Buckley *et al.*, Eur. Phys. J. C **65**, 331 (2010); R. Field and R. C. Group, arXiv:hep-ph/0510198. The difference between the *ACpro* and *Apro* tunes is used to estimate the systematic uncertainty related to color reconnection.
[21] G. Corcella *et al.*, J. High Energy Phys. **01**, 010 (2001).
[22] J. Pumplin *et al.*, J. High Energy Phys. **07**, 012 (2002); D. Stump *et al.*, J. High Energy Phys. **10**, 046 (2003).
[23] L. Lyons, D. Gibaut, and P. Clifford, Nucl. Instrum. Methods Phys. Res. A **270**, 110 (1988); A. Valassi, Nucl. Instrum. Methods Phys. Res. A **500**, 391 (2003).